AIP | APL Materials

Polymer-based solar cells having an active area of 1.6 cm2 fabricated via spray coating

N. W. Scarratt, J. Griffin, T. Wang, Y. Zhang, H. Yi, A. Iraqi, and D. G. Lidzey

Citation: APL Mater. **3**, 126108 (2015); doi: 10.1063/1.4937553
View online: http://dx.doi.org/10.1063/1.4937553
View Table of Contents: http://scitation.aip.org/content/aip/journal/aplmater/3/12?ver=pdfcov
Published by the AIP Publishing

Polymer-based solar cells having an active area of 1.6 cm^2 fabricated via spray coating

N. W. Scarratt,[1] J. Griffin,[1] T. Wang,[1,2] Y. Zhang,[1] H. Yi,[3] A. Iraqi,[3] and D. G. Lidzey[1,a]

[1]*Department of Physics and Astronomy, University of Sheffield, Sheffield S3 7RH, United Kingdom*
[2]*School of Materials Science and Engineering, Wuhan University of Technology, Wuhan 430070, China*
[3]*Department of Chemistry, University of Sheffield, Sheffield S3 7HF, United Kingdom*

(Received 25 August 2015; accepted 30 November 2015; published online 23 December 2015)

We demonstrate the fabrication of polymer solar cells in which both a PEDOT:PSS hole transport and a PCDTBT:$PC_{71}BM$ photoactive layer are deposited by spray-casting. Two device geometries are explored, with devices having a pixel area of 165 mm^2 attaining a power conversion efficiency of 3.7%. Surface metrology indicates that the PEDOT:PSS and PCDTBT:$PC_{71}BM$ layers have a roughness of 2.57 nm and 1.18 nm over an area of 100 μm^2. Light beam induced current mapping reveals fluctuations in current generation efficiency over length-scales of ~2 mm, with the average photocurrent being 75% of its maximum value. [http://dx.doi.org/10.1063/1.4937553]

As the energy demands of society increase, new carbon-neutral energy sources are required. Organic photovoltaics (OPVs) are one such energy source, offering the potential of a low-cost, light-weight, and low embodied-energy alternative to conventional solar cells.[1]

Most prototype OPV devices are fabricated by spin-coating onto relatively small substrates. While spin-coating is a powerful tool to deposit materials in a controllable and accurate fashion, it is a relatively slow and un-scalable process. For a technology such as OPV to make a transition to commercial manufacture, it is necessary to demonstrate the fabrication of devices using scalable deposition techniques. Several printing and coating techniques have been used in the scale up of OPVs. Printing techniques such as gravure,[2] screen,[3] slot die,[4] and inkjet[5] have all demonstrated compatibility with OPV layers.[6] Of the many roll-to-roll compatible processing methods currently being researched, spray coating is gaining increased attention. This technique combines rapid deposition-speeds and can be used to deposit a variety of functional materials from a range of inks having different physical properties.

Airbrush spray coating has been used to deposit PEDOT:PSS[7] hole transport layers, P3HT:PCBM[8–11] photoactive layers, and in some cases both layers sequentially.[12–15] Notably, Park *et al.* created OPV devices having a size of 12.5 cm^2 and a power conversion efficiency (PCE) of 1.68% from spray cast P3HT:PCBM using Al grids placed throughout the transparent anode.[9] Hoth *et al.* spray cast both PEDOT:PSS and P3HT:PCBM layers and achieved a PCE of 2.7% from devices having an active area of 0.11 cm^2. We have previously demonstrated the spray coating of blends of carbazole-based polymers and PCBM as photoactive layers.[16] The resultant devices had comparable efficiency to devices in which the active layer was deposited by spin-casting. Follow-up work demonstrated that both the photoactive layer and a hole-transporting molybdenum oxide hole-transport layer could be deposited by spray-coating, permitting spin-coating to be removed from the device fabrication process.[17] In other work, spray-coating has been used to spray-cast perovskite films with promising efficiencies obtained.[18]

[a]Email: d.g.lidzey@sheffield.ac.uk

In this paper, we explore a limited scale-up of OPVs by ultra-sonic spray-coating, and critically, we present a process that allows us to spray-coat both the polymer fullerene active layer and the PEDOT:PSS hole extracting anode. Using the well-known donor-acceptor polymer poly[N-9′-heptadecanyl-2,7-carbazole-alt-5,5-(4′,7′-di-2-thienyl-2′,1′,3′-benzothiadiazole)] (PCDTBT) and acceptor [6,6]-phenyl-C71-butyric acid methyl ester ($PC_{71}BM$), we create fully spray-cast devices having an active area of 4 and 165 mm^2 having a PCE of 4.9% and 3.7%, respectively. We discuss the origin for the reduction in PCE on scale-up and comment on the prospects for this technology.

The devices fabricated are based on the conjugated-polymer PCDTBT. This material has a deep HOMO level, resulting in increased stability against oxidation.[19–21] This is a widely used donor polymer in organic photovoltaics, with reported power conversion efficiencies exceeding 7%.[22–26] Thin-films of PCDTBT are relatively amorphous and thus solution-based deposition techniques that incorporate relatively rapid drying times are possible without significantly compromising the charge transport properties of the active layer.[27]

Figure 1 shows a schematic of the ultrasonic spray coating system used in this work (a PRISM 300 ultrasonic spray coater supplied by Ultrasonic Systems, Inc.). Here, the solution of interest is fed through a tube at a controlled pressure onto a tip vibrating at ultra-sonic frequency. The vibration of the tip breaks the solution into droplets forming a uniform spray mist that is carried onto a surface using a continuous flow of nitrogen, with the size of the droplets determined by the frequency of vibration of the tip and the surface tension of the solution. This process is unlike traditional aerosol spray-coating wherein the droplet size is determined by the pressure of a solution passing through a nozzle. Ultra-sonic spray-coating thus permits control over the volume of solution deposited without altering the size of the droplets that reach the substrate. In the system used, the spray head is attached to a computer-controlled gantry that controls the motion of the head above the surface. The substrates on which the film is deposited are placed on a hotplate to allow the film drying-time to be controlled. The volume of solution that is deposited onto a substrate can be altered by control of the lateral-speed and height of the spray head, together with the gas pressure used to carry the droplets. By optimising parameter space, it is possible to deposit a film having a desired thickness with a single pass of the spray head.

The structure of the devices explored is shown schematically in Figure 2(a) and is based around the geometry ITO/PEDOT:PSS(30 nm)/PCDTBT:$PC_{71}BM$(55 nm)/Ca(5 nm)/Al(100 nm). In all cases, devices were fabricated onto a glass substrate coated with a pre-patterned ITO anode, with the overlapping pattern of the anode and cathode determining the resultant pixel size. We have explored two different device designs as shown schematically in Figures 2(b) and 2(c). Here, the pixel area ranges from 4 mm^2 (part (b)) to 165 mm^2 (parts (c) and (d)). In each case, the dimensions and area of the different substrates and pixels are detailed in Table I.

To fabricate the devices, a PEDOT:PSS solution (AI-4083)was first filtered through a 0.45 μm polyvinylidenedifluoride filter into a pre-cleaned glass vial. This material is supplied in an aqueous

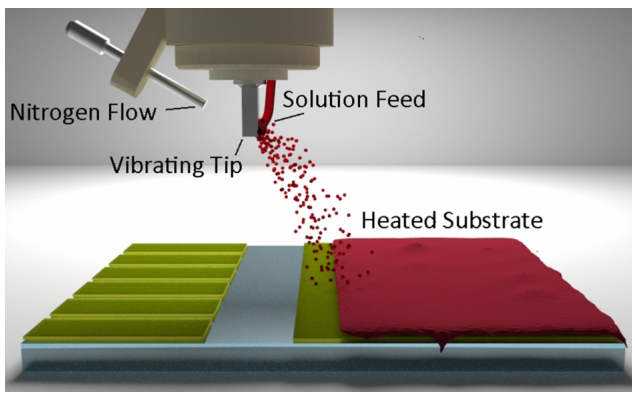

FIG. 1. A schematic of the ultrasonic spray coater.

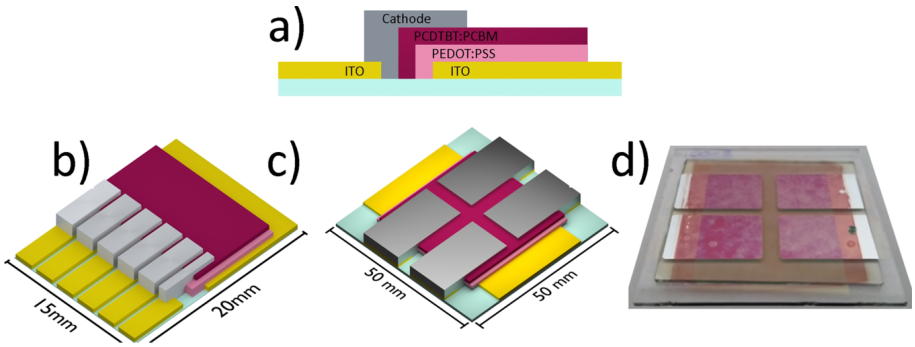

FIG. 2. Part (a) shows the device architecture, with parts (b) and (c) showing orthographic diagrams of device architectures used in this work. Here, part (b) shows the small-area (4 mm^2) six pixel substrate, with part (c) showing the large-area (165 mm^2) four pixel devices. Part (d) shows an image of a device fabricated using the architecture shown in (c).

dispersion that has a high surface tension and forms droplets having a high initial contact angle of 19.6°on ITO. For this reason, it was found that AI-4083 could not be spray-cast on ITO without undergoing dewetting. It was found (as shown in the previous reports) that the addition of isopropyl alcohol (IPA) to a PEDOT:PSS solution aids wetting[12] when cast on an ITO surface; however, such films were not found to be particularly uniform. To address this issue, a range of processing additives were explored and it was found that a continuous, uniform film could be formed by spray coating by mixing the AI-4083 with IPA and ethylene glycol (EG) at a solution ratio of 1:8:1. Onto this, a polymer:fullerene active layer was spray-cast from an ink based on a (1:4) blend of PCDTBT:$PC_{71}BM$ in chlorobenzene (total solid concentration of 8 mg ml^{-1}), with the PCDTBT used being synthesised as reported previously by Yi *et al.*[28] (M_w = 34.6 kDa, PDI = 2.33). A series of spin-cast control devices were also explored. Here, to obtain a film having the desired film thickness, it was necessary to increase the solid concentration of the ink to 25 mg ml^{-1}.

Device preparation commenced by cleaning the ITO substrates via sonication for 5 min successively in sodium hydroxide, Hellmanex, hot deionised water, and IPA with a dunk rinse in hot DI water between the sodium hydroxide and Hellmanex stages. The substrates were then dried using a nitrogen jet and placed on a hot plate for 10 min. Sequential spray coating of both the PEDOT:PSS and PCDTBT:$PC_{71}BM$ layers was performed in air onto substrates held at a temperature of 20 °C and 40 °C, respectively, with the spray-head to substrate distance being 65 mm. In the case of the PEDOT:PSS layer, substrates were then transferred to a hotplate held at 120 °C to evaporate the higher boiling point ethylene glycol. Other process conditions were similar to those described in our previous work.[16] The coated substrates were then transferred to a nitrogen-filled glovebox connected to a vacuum evaporation chamber. A 5 nm thick calcium electron transport layer was deposited on the surface of the PCDTBT:$PC_{71}BM$, followed by a 100 nm thick aluminium cathode. After cathode deposition, the devices were removed from the vacuum chamber and encapsulated using a glass slip and UV epoxy resin.

Devices were tested using a Newport 92261A-1000 AM1.5 solar simulator and a Keithley 2400 source meter. The solar simulator power was adjusted to 100 $mWcm^{-2}$ using a NREL

TABLE I. Substrate dimensions, pixel number, and active areas for device architectures used in this work.

Architecture name	Substrate dimensions (mm × mm)	Pixel dimensions (mm × mm)	Pixel area (mm^2)	Pixels per substrate
Small six	20 × 15	2 × 2	4	6
Large four	50 × 50	12.7 × 13	165	4

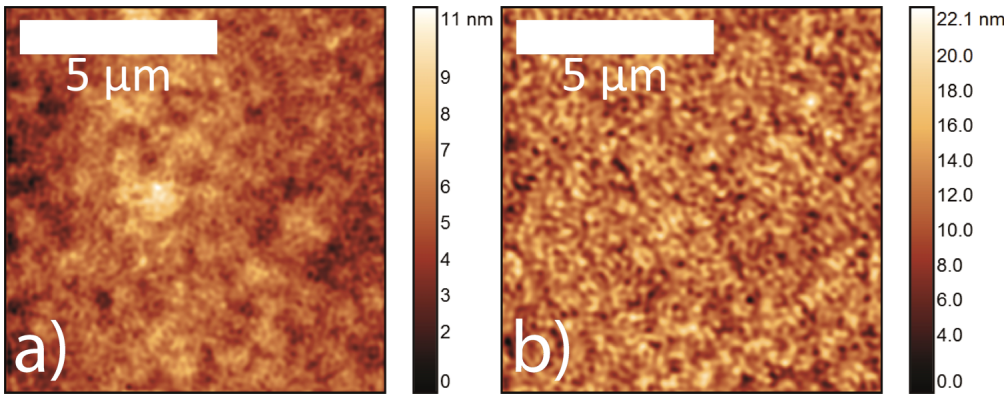

FIG. 3. AFM measurement of (a) a spray-cast PEDOT:PSS film with a rms roughness of 2.57 nm. The film was deposited from a solution of PEDOT:PSS, IPA, and ethylene glycol in a 1:8:1 ratio. Part (b) shows a PCDTBT:PC_{71} BM film with a rms roughness of 1.18 nm. The film was spray-cast on to a PEDOT:PSS film from a chlorobenzene solution at a ratio of 1:4.

calibrated silicon diode and a shadow mask was used to define the illuminated region. Atomic force microscopy was performed using a Veeco Dimension 3100 operating in tapping mode. The uniformity of the photocurrent generation was explored using light beam induced current (LBIC) mapping. Here, light from a 405 nm (4 mW) laser diode was focused via a 50X Mitutoyo infinity-corrected objective lens to a spot on the OPV surface having a diameter of <5 μm. The OPV was mounted on a computer-controlled xy-stage and moved in a raster pattern with 100 μm steps over the (x,y) plane. The photocurrent was measured using a lock in amplifier and an optical chopper to recover the signal.

In Figure 3(a), we show an AFM measurement of a PEDOT:PSS film created by spray coating. Image analysis reveals that this film has a root-mean-square (rms) roughness of 2.57 nm and a uniformity of ±12 nm over an area of 100 μm^2, thus acting as a highly homogeneous and smooth hole-extraction film on which to deposit the photoactive layer. It was found that the inclusion of the EG processing additive resulted in a significant increase in the conductivity of the PEDOT:PSS film, with the electrical conductivity of the spin and spray-cast films being 0.0023 and 4.45 S cm^{-1}, respectively. This agrees with the previous reports of the use of EG resulting in a reconfiguration of molecular structure in the PEDOT:PSS film and has been proposed as a route to creating an ITO-free electrode.[29] The optical transmittance of the spray-cast PEDOT:PSS film is displayed in the supplementary material (Figure S1).[34]

The operational metrics for devices in which both the PEDOT:PSS and active layer were fabricated by spray coating are shown in Table II. Here, data are included for pixels having an active area of both 4 mm^2 and 165 mm^2. Data are also included recorded from control devices in which both the PEDOT:PSS and active layer were fabricated by spin coating. The *JV* curves for a typical spray-cast device are plotted in Figure 4. It can be seen that all devices are characterised by a relatively similar open circuit voltage (V_{oc}), with the maximum efficiency of the 4 mm^2 active area devices prepared by either spin or spray coating both being 4.9% (within experimental uncertainty). This indicates that spray-coating is an effective method to prepare both the active and hole-extracting layers of an OPV device. Notably however, it can be seen that the short circuit

TABLE II. Device metrics for spray-cast devices with varying area. A spin-cast reference is included.

Pixel size (mm^2)	Deposition technique	PCE (%)	Max PCE (%)	Device number	FF (%)	J_{sc} (mA cm^{-2})	V_{oc} (V)	R_{shunt} (Ω cm^2)	R_{series} (Ω cm^2)
4	Spin	4.8 ± 0.1	4.9	6	60	−8.8	0.91	737	11
4	Spray	4.1 ± 0.8	4.9	6	50	−9.6	0.87	452	17.1
165	Spray	3.4 ± 0.3	3.7	4	45	−8.6	0.87	319	31.3

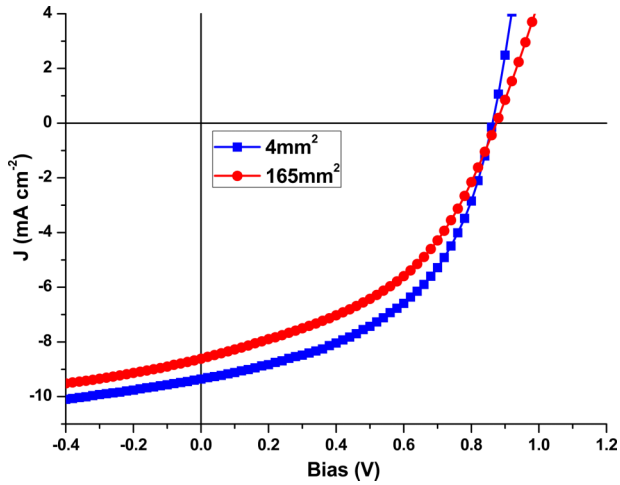

FIG. 4. Current-voltage curves of spray-cast devices using the small six and large four architectures.

current density and fill factor are reduced in the devices having a pixel area of 165 mm^2, with a maximum PCE of 3.4% obtained. As V_{oc} is primarily affected by the work function of the electrodes and the donor-acceptor energy difference,[30] such properties are expected to be independent of device area.[31] To understand the origin of the reduced *FF*, we have measured the resistance of the different uncoated ITO substrates between the centre of the pixel and the anode contact at the substrate edge. It was found that for the small area device, there was an effective series resistance of 29 Ω, a value that increased to 40 Ω for the large area substrates. This 1.4 times increase in resistance occurred as a result of the longer path-length between pixel and contact, being 10 mm and 19 mm in the small and large-area pixel devices, respectively. From our *JV* curves (data in Table II), we determine an increase in series resistance between small and large area devices of ~1.8 times, a value commensurate with our resistance measurements. We, therefore, ascribe the loss in *FF* to the increased series resistance of the ITO anode, a result in agreement with the literature.[32] We note that such losses can be reduced by the use of metallic grids or bus-bars.[33] Despite this reduced efficiency, such devices have comparable performance to many other reports of spray-cast OPV devices reported in the literature, and critically we believe that these are the largest OPVs yet reported in which the PEDOT:PSS hole transport layer and the photoactive layer are both spray coated.

To investigate the uniformity of current generation across the cell, LBIC maps were recorded from spray-cast devices pixels having an active area of 165 mm^2. Figure 5(a) shows a typical LBIC image, with part (b) showing a histogram summarising the distribution of the photocurrent measured across the device. It can be seen that there is some fluctuation in the photocurrent across the device, with the average photocurrent determined being around 75% of the maximum generated current. Analysis of the image indicates that photocurrent fluctuations occur over mm length-scales. Despite the fact that our films are smooth over areas of 100 μm^2, there is significant inhomogeneity in film thickness over longer length-scales. This conclusion is confirmed in part (c), where we plot a profilometry scan recorded from the surface of a typical spray-cast PCDTBT:PC$_{70}$BM film. Here, fluctuations of around 30 nm are seen over length-scales of ~2 mm. We speculate that this inhomogeneity results from turbulence in the gas stream during spray-casting.

We have, therefore, investigated the performance of organic photovoltaic cells with spray-cast hole transport and photoactive layers. To obtain a homogeneous film of the hole-transporting polymer PEDOT:PSS, it was found necessary to dilute the PEDOT:PSS solution using the solvent IPA and use the process additive ethylene glycol. Using such a spray-cast anode, the fabrication of OPV devices was demonstrated having a maximum pixel size of 165 mm^2 and a PCE of 3.7%. Our work further demonstrates the feasibility of OPV scale up by spray-coating and indicates that this technique can be used to create relatively efficient devices.

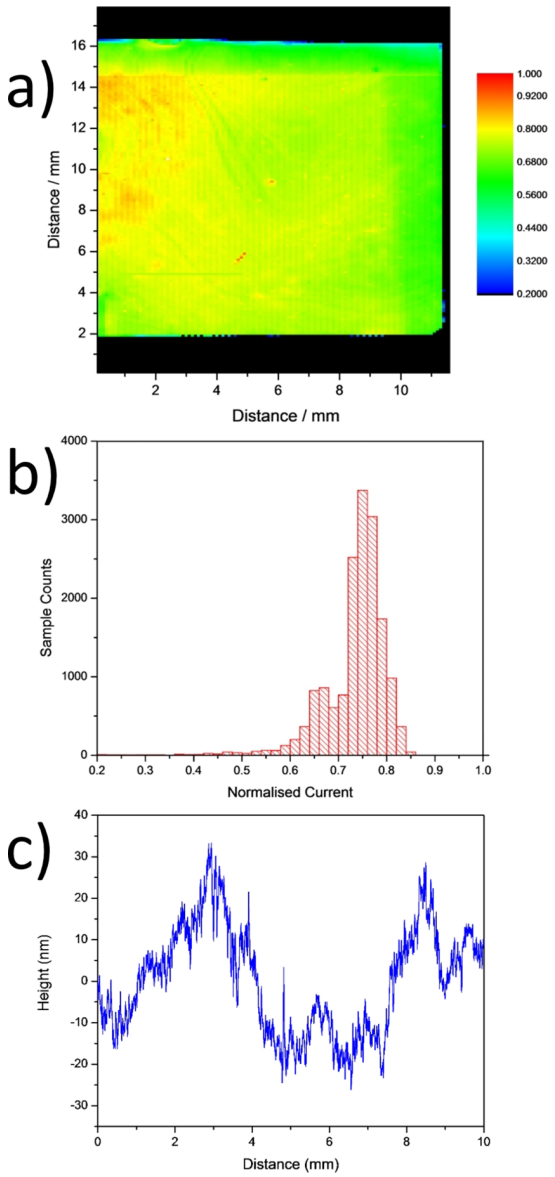

FIG. 5. Part (a) shows light beam induced current map of a large four pixel, with part (b) showing a histogram of the photocurrent data shown in part (a). Part (c) shows a profilometry scan of a spray cast PCDTBT:$PC_{70}BM$ layer over a length of 10 mm.

We gratefully thank the UK EPSRC for funding this work via research Grant Nos. EP/I028641/1 and EP/J017361/1. N.W.S. thanks the EPSRC for the award of a DTG studentship, and Y.Z. thanks the University of Sheffield for a Ph.D Scholarship.

[1] A. J. Pearson, T. Wang, and D. G. Lidzey, "The role of dynamic measurements in correlating structure with optoelectronic properties in polymer: Fullerene bulk-heterojunction solar cells," Rep. Prog. Phys. **76**, 022501 (2013).
[2] P. Kopola *et al.*, "Gravure printed flexible organic photovoltaic modules," Sol. Energy Mater. Sol. Cells **95**, 1344–1347 (2011).
[3] F. C. Krebs, J. Alstrup, H. Spanggaard, K. Larsen, and E. Kold, "Production of large-area polymer solar cells by industrial silk screen printing, lifetime considerations and lamination with polyethyleneterephthalate," Sol. Energy Mater. Sol. Cells **83**, 293–300 (2004).
[4] F. C. Krebs, "Polymer solar cell modules prepared using roll-to-roll methods: Knife-over-edge coating, slot-die coating and screen printing," Sol. Energy Mater. Sol. Cells **93**, 465–475 (2009).
[5] C. N. Hoth, S. A. Choulis, P. Schilinsky, and C. J. Brabec, "High photovoltaic performance of inkjet printed polymer: Fullerene blends," Adv. Mater. **19**, 3973–3978 (2007).

[6] R. R. Søndergaard, M. Hösel, and F. C. Krebs, "Roll-to-Roll fabrication of large area functional organic materials," J. Polym. Sci., Part B: Polym. Phys. **51**, 16–34 (2013).
[7] R. J. Peh, Y. Lu, F. Zhao, C.-L. K. Lee, and W. L. Kwan, "Vacuum-free processed transparent inverted organic solar cells with spray-coated PEDOT:PSS anode," Sol. Energy Mater. Sol. Cells **95**, 3579–3584 (2011).
[8] C. Girotto, B. P. Rand, J. Genoe, and P. Heremans, "Exploring spray coating as a deposition technique for the fabrication of solution-processed solar cells," Sol. Energy Mater. Sol. Cells **93**, 454–458 (2009).
[9] S.-Y. Park *et al.*, "Spray-coated organic solar cells with large-area of 12.25 cm^2," Sol. Energy Mater. Sol. Cells **95**, 852–855 (2011).
[10] G. Susanna *et al.*, "Airbrush spray-coating of polymer bulk-heterojunction solar cells," Sol. Energy Mater. Sol. Cells **95**, 1775–1778 (2011).
[11] D. J. Vak *et al.*, "Fabrication of organic bulk heterojunction solar cells by a spray deposition method for low-cost power generation," Appl. Phys. Lett. **91**, 081102 (2007).
[12] C. Girotto, D. Moia, B. P. Rand, and P. Heremans, "High-performance organic solar cells with spray-coated hole-transport and active layers," Adv. Funct. Mater. **21**, 64–72 (2011).
[13] C. N. Hoth *et al.*, "Topographical and morphological aspects of spray coated organic photovoltaics," Org. Electron. **10**, 587–593 (2009).
[14] Y.-F. Lim *et al.*, "Spray-deposited poly(3,4-ethylenedioxythiophene): Poly(styrenesulfonate) top electrode for organic solar cells," Appl. Phys. Lett. **93**, 193301 (2008).
[15] S.-I. Na *et al.*, "Fully spray-coated ITO-free organic solar cells for low-cost power generation," Sol. Energy Mater. Sol. Cells **94**, 1333–1337 (2010).
[16] T. Wang *et al.*, "Fabricating high performance, donor-acceptor copolymer solar cells by spray-coating in air," Adv. Energy Mater. **3**, 505–512 (2013).
[17] J. Griffin *et al.*, "Organic photovoltaic devices incorporating a molybdenum oxide hole-extraction layer deposited by spray-coating from an ammonium molybdate tetrahydrate precursor," Org. Electron. **15**, 692–700 (2014).
[18] A. Barrows *et al.*, "Efficient planar heterojunction mixed-halide perovskite solar cells deposited via spray-deposition," Energy Environ. Sci. **7**, 2944 (2014).
[19] T.-Y. Chu *et al.*, "Highly efficient polycarbazole-based organic photovoltaic devices," Appl. Phys. Lett. **95**, 063304 (2009).
[20] D. M. De Leeuw, M. M. J. Simenon, A. R. Brown, and R. E. F. Einerhand, "Stability of n-type doped conducting polymers and consequences for polymeric microelectronic devices," Synth. Met. **87**, 53–59 (1997).
[21] E. Bovill *et al.*, "The role of the hole-extraction layer in determining the operational stability of a polycarbazole:fullerene bulk-heterojunction photovoltaic device," Appl. Phys. Lett. **106**, 073301 (2015).
[22] T.-Y. Chu *et al.*, "Morphology control in polycarbazole based bulk heterojunction solar cells and its impact on device performance," Appl. Phys. Lett. **98**, 253301 (2011).
[23] Y. Sun *et al.*, "Efficient air-stable bulk heterojunction polymer solar cells using MoO(x) as the anode interfacial layer," Adv. Mater. **23**, 2226–2230 (2011).
[24] W. Kim *et al.*, "Polymer bulk heterojunction solar cells with PEDOT:PSS bilayer structure as hole extraction layer," ChemSusChem **6**, 1070–1075 (2013).
[25] D. H. Wang *et al.*, "Transferable graphene oxide by stamping nanotechnology: Electron-transport layer for efficient bulk-heterojunction solar cells," Angew. Chem., Int. Ed. **52**, 2874–2880 (2013).
[26] D. H. Wang *et al.*, "Enhanced power conversion efficiency in PCDTBT/PC70BM bulk heterojunction photovoltaic devices with embedded silver nanoparticle clusters," Adv. Energy Mater. **1**, 766–770 (2011).
[27] T. Wang *et al.*, "Correlating structure with function in thermally annealed PCDTBT: PC70BM photovoltaic blends," Adv. Funct. Mater. **22**, 1399–1408 (2012).
[28] H. Yi *et al.*, "Carbazole and thienyl benzo[1,2,5]thiadiazole based polymers with improved open circuit voltages and processability for application in solar cells," J. Mater. Chem. **21**, 13649 (2011).
[29] J. Ouyang, C.-W. Chu, F.-C. Chen, Q. Xu, and Y. Yang, "High-conductivity poly(3,4-ethylenedioxythiophene): Poly(styrene sulfonate) film and its application in polymer optoelectronic devices," Adv. Funct. Mater. **15**, 203–208 (2005).
[30] V. D. Mihailetchi, P. W. M. Blom, J. C. Hummelen, and M. T. Rispens, "Cathode dependence of the open-circuit voltage of polymer: Fullerene bulk heterojunction solar cells," J. Appl. Phys. **94**, 6849 (2003).
[31] W.-I. Jeong, J. Lee, S.-Y. Park, J.-W. Kang, and J.-J. Kim, "Reduction of collection efficiency of charge carriers with increasing cell size in polymer bulk heterojunction solar cells," Adv. Funct. Mater. **21**, 343–347 (2011).
[32] S. Choi, W. J. Potscavage, and B. Kippelen, "Area-scaling of organic solar cells," J. Appl. Phys. **106**, 054507 (2009).
[33] A. Armin *et al.*, "Efficient, large area, and thick junction polymer solar cells with balanced mobilities and low defect densities," Adv. Energy Mater. **5**, 1401221 (2015).
[34] See supplementary material at http://dx.doi.org/10.1063/1.4937553 for optical transmission of the PEDOT:PSS film.